

# Identification of Human miRNA Biomarkers Targeting the SARS-CoV-2 Genome

Indrajit Saha,\* Nimisha Ghosh,\*<sup>⊥</sup> and Dariusz Plewczynski\*Cite This: *ACS Omega* 2022, 7, 46411–46420

Read Online

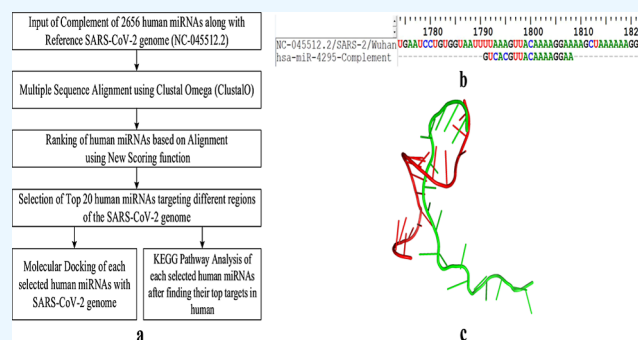
ACCESS |

Metrics &amp; More

Article Recommendations

Supporting Information

**ABSTRACT:** SARS-CoV-2 poses a great challenge toward mankind, majorly due to its evolution and frequently occurring variants. On the other hand, in human hosts, microRNA (miRNA) plays a vital role in replication and propagation during a viral infection and can control the biological processes. This may be essential for the progression of viral infection. Moreover, human miRNAs can play a therapeutic role in treatment of different viral diseases by binding to the target sites of the virus genome, thereby hindering the essential functioning of the virus. Motivated by this fact, we have hypothesized a new approach in order to identify human miRNAs that can target the mRNA (genome) of SARS-CoV-2 to degrade their protein synthesis. In this regard, the multiple sequence alignment technique Clustal Omega is used to align a complement of 2656 human miRNAs with the SARS-CoV-2 reference genome (mRNA). Thereafter, ranking of these aligned human miRNAs is performed with the help of a new scoring function that takes into account the (a) total number of nucleotide matches between the human miRNA and the SARS-CoV-2 genome, (b) number of consecutive nucleotide matches between the human miRNA and the SARS-CoV-2 genome, (c) number of nucleotide mismatches between the human miRNA and the SARS-CoV-2 genome, and (d) the difference in length before and after alignment of the human miRNA. As a result, from the 2656 ranked miRNAs, the top 20 human miRNAs are reported, which are targeting different coding and non-coding regions of the SARS-CoV-2 genome. Moreover, molecular docking of such human miRNAs with virus mRNA is performed to verify the efficacy of the interactions. Furthermore, 4 miRNAs out of the top 20 miRNAs are identified to have the seed region. In order to inhibit the virus, the key human targets of the seed regions may be targeted. Repurposable drugs like carfilzomib, bortezomib, hydralazine, and paclitaxel are identified for such purpose.



## INTRODUCTION

MicroRNAs are small non-coding molecules of length 18–25 nucleotides which act as gene regulators by targeting 3′-UTR, 5′-UTR, and coding regions of mRNA<sup>1</sup> and play an important role in life processes.<sup>2</sup> miRNA is also known to be involved in many physiological processes and is also important in cell development.<sup>3</sup> Inside the human body, there are more than 2000 precursor miRNAs that play numerous roles within the host body.<sup>4–6</sup> Although it is a challenging task to figure out human miRNA and virus mRNA interactions, it is well established that human miRNAs play vital role in stopping the replications and propagation of the virus during a viral infection by binding to the virus genome and controlling the biological processes. Therefore, human miRNAs can regulate the infection through complex regulatory pathways.<sup>7</sup> However, it also needs to be pointed out that viruses can also use miRNAs for their survival by incorporating the miRNA seeding region in their genome. To stabilize their genome and prevent degradation, some viruses use host-derived miRNAs.<sup>7,8</sup> miR-122 directly binds to the 5′-UTR of HCV and stabilizes the RNA to promote viral

reflection.<sup>9</sup> Herpes viruses also use miRNAs to repress cellular targets to modulate host cells.<sup>10</sup>

miRNAs often lead to mRNA degradation by binding to the complementary regions of specific messenger RNAs in order to regulate the functioning of mRNAs.<sup>11</sup> As a consequence, it plays an eccentric role in the human genome by regulating the protein-coding genes. On the other hand, a virus relies heavily on the metabolism of the host body in order to provide a suitable environment for viral infection and infectivity.<sup>12</sup> It is to be noted that virus infections has a direct effect on miRNA profiling. Li et al.<sup>13</sup> conducted similar experiment on HCV infection with microarray analysis. As a result, they found that miR-25, miR-130a/b, and let-7a down-regulated miRNAs have a direct impact

Received: August 9, 2022

Accepted: October 6, 2022

Published: December 5, 2022



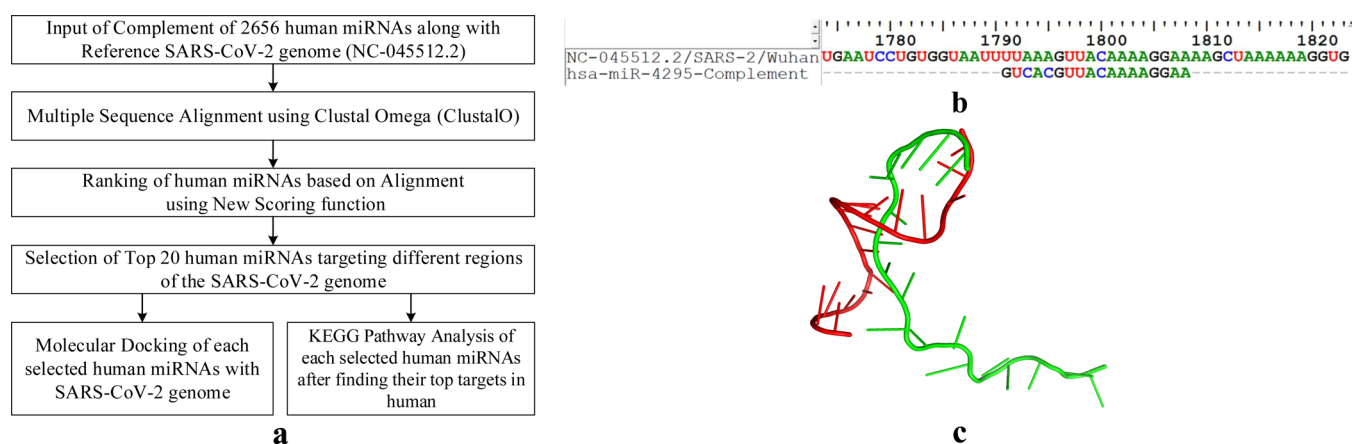


**Figure 1.** Graphical abstract to visualise (a) flowchart of the work (b) aligned complement of the human miRNA hsa-miR-4029 with the reference SARS-CoV-2 genome (c) docked pose of the hsa-miR-4029 miRNA and virus mRNA (genome).

on the virus genome in the culture of liver tissues. Moreover, in the case of enterovirus 71 infection,<sup>14</sup> miR-141 was found to be affected in cells. Similarly, in miRNA profiling of the Newcastle disease virus done with the help of microarray-based analysis, miR-485-5p was found to be up-regulated, and a similar trend was also seen in the case of influenza virus.<sup>15</sup> In addition to this, microarray analysis of miRNAs in the case of IAV infected lungs of mice discovered miR-144 as the up-regulated miRNA which resulted in increased virion production in cells.<sup>16</sup> With the motivation that RNA viruses can encode miRNAs, which can modulate host gene expression, Roy et al.<sup>17</sup> predicted viral miRNA-like sequences for SARS-CoV-2, MERS-CoV, and SARS-CoV. They also analyzed sequence reciprocity and used bioinformatics tools and machine learning algorithms like Naive Bayes to identify SARS-CoV-2-encoded possible miRNA-human gene interactions. In ref 18, the authors used a computational approach to screen various miRNAs targeted against the ORF8 gene of SARS-CoV-2. Their results indicated that miRNAs targeting ORF8 had agreeable shape complementarity as well as they were successfully docked with the ORF7a gene. Islam et al.<sup>19</sup> performed an in silico analysis to hypothesize that the Chikungunya virus may create miRNAs which target host genes for their survival. In this regard, they identified many such miRNAs using a bioinformatics approach. Thereafter, they predicted the host genes targeted by such miRNAs. In ref 20, Haldar et al. used network analysis to correlate the host protein BCL2L1 with the miRNA miR-23b. According to their study, miRNAs can inhibit viral infection by increasing the production of IFN  $\alpha/\beta$  or help the virus to avoid host immune response by suppressing the same.

On the other hand, it is found that host miRNAs also block the virus replication due to increased levels of a specific miRNA or by binding to the viral genome in different fashions.<sup>21</sup> In this regard, miR-296-5p was found to be targeting the capsid protein of the enterovirus 71 genome in the form of a viral response.<sup>21</sup> Similarly, in ref 22, the case of CVB3 (coxsackievirus B3), miR-342-5p was found to be the key in degrading the virus through targeting the 2C-coding region of the viral mRNA. miR-221 and miR-222 are known to limit human immunodeficiency virus type 1 (HIV-1) propagation and production in the human body.<sup>23</sup> The first evidence that a miRNA, miR-548g-3p, could suppress dengue virus (DENV) multiplication by directly binding to the virus genome was reported in ref 24. Similarly, Betancur and Inchima<sup>25</sup> found miRNAs like miR-133a, miR-

484, and miR-744 targeting the DENV genome by inhibiting the virus replication. Another study found miR-252 as highly suppressing the DENV-2 genome by targeting the coding region of the envelope protein of the DENV-2 RNA genome.<sup>26</sup>

Moreover, human miRNAs play many different and important roles in SARS-CoV-2<sup>27</sup> infections by inhibiting viral replication, blocking cellular receptors, and deactivating the functioning of viral proteins. Ref 12 reports a study where the expression analysis of the human miRNAs was done, and it was found that an increased expression of miR-1037-3p leads to the inhibition of the replication of the SARS-CoV-2 genome. The structural and non-structural proteins of SARS-CoV-2 are responsible for the entry, replication, and infection of the virus in a human host. In order to stop this, for example, miR-190a-5p targets the coding region of ORF6 in the SARS-CoV-2 genome. Therefore, these miRNAs can be considered as an innate antiviral defense system since SARS-CoV-2 replicates and inhibit the immune system by decreasing the cellular miRNAs. Moreover, in another study conducted by Rad Sm et al.,<sup>28</sup> it was demonstrated that miR-29b-3p, miR-338-3p, miR-4661-3p, miR-4761-5p, and miR-4793-5p may act against the S protein of the SARS-CoV-2 genome. Arisan et al.<sup>29</sup> reported that miR-8066 could act against the SARS-CoV-2 nucleocapsid gene, which encodes a basic RNA-binding protein. Therefore, targeting this gene can reduce or block the assembly and production of the virus genome. On the other hand, it is known that patients suffering from diseases such as diabetes and cardiovascular disease have a high expression of ACE2 receptors; hence, blocking the binding mechanism of ACE2 and the spike protein with the miRNA can also be a potential treatment for the more vulnerable patients.<sup>30</sup> Therefore, it is highly important to identify such miRNAs that can help in reducing the impact of SARS-CoV-2.

Taking cues from the above literature, we have hypothesized a new approach in order to identify putative human miRNAs that can target the mRNA (genome) of SARS-CoV-2 to degrade its protein synthesis. In this regard, the multiple sequence alignment technique Clustal Omega is used to align a complement of 2656 human miRNAs with the SARS-CoV-2 reference genome (mRNA). Thereafter, ranking of these aligned human miRNAs is done with the help of a new scoring function which takes into account (a) the total number of nucleotide matches between the human miRNA and the SARS-CoV-2 genome, (b) number of consecutive nucleotide matches between the human miRNA and the SARS-CoV-2 genome,

Table 1. Top 20 Human miRNAs Targeting SARS-CoV-2 Genome in Different Coding and Non-Coding Regions

| human miRNA     | total number of nucleotide matches (m) | number of consecutive nucleotide matches (c) | number of nucleotide mismatches (n) | expanded length of human miRNA after alignment ( $\lambda$ ) | length of human miRNA ( $\delta$ ) | score (S) | aligned SARS-CoV-2 genome with human miRNA |                | coding and non-coding region | genomic coverage (%) |
|-----------------|--|--|-------------------------------------|--|------------------------------------|-----------|--|----------------|------------------------------|----------------------|
|                 |  |  |                                     |  |                                    |           | start coordinate                           | end coordinate |                              |                      |
| hsa-miR-4295    | 15                                     | 13   | 3                                   | 18   | 18                                 | 16.370    | 1791                                       | 1808           | NSP2                         | 99.885               |
| hsa-miR-3611    | 17                                     | 14   | 4                                   | 21   | 21                                 | 16.024    | 4936                                       | 4956           | NSP3                         | 99.885               |
| hsa-miR-145-3p  | 17                                     | 15   | 5                                   | 22   | 22                                 | 15.419    | 17968                                      | 17989          | helicase                     | 99.693               |
| hsa-miR-6857-3p | 17                                     | 11   | 4                                   | 21   | 21                                 | 15.078    | 929  | 949            | NSP2                         | 99.510               |
| hsa-miR-548f-3p | 15                                     | 12   | 4                                   | 19   | 19                                 | 14.928    | 4032                                       | 4050           | NSP3                         | 99.596               |
| hsa-miR-5694    | 17                                     | 10   | 4                                   | 21   | 21                                 | 14.704    | 21668                                      | 21688          | spike                        | 99.865               |
| hsa-miR-3158-5p | 17                                     | 10   | 4                                   | 21   | 21                                 | 14.704    | 29239                                      | 29259          | nucleocapsid                 | 99.068               |
| hsa-miR-4678    | 17                                     | 11   | 5                                   | 22   | 22                                 | 14.203    | 1511                                       | 1532           | NSP2                         | 99.097               |
| hsa-miR-2355-3p | 17                                     | 11   | 5                                   | 22   | 22                                 | 14.203    | 10013                                      | 10034          | NSP4                         | 99.126               |
| hsa-miR-1306-3p | 14                                     | 10   | 4                                   | 18   | 18                                 | 13.943    | 16745                                      | 16762          | helicase                     | 99.750               |
| hsa-miR-5582-5p | 16                                     | 13   | 6                                   | 22   | 22                                 | 13.905    | 21948                                      | 21969          | spike                        | 99.712               |
| hsa-miR-3121-3p | 17                                     | 10   | 5                                   | 22   | 22                                 | 13.829    | 2215                                       | 2236           | NSP2                         | 99.750               |
| hsa-miR-4753-5p | 17                                     | 10   | 5                                   | 22   | 22                                 | 13.829    | 11179                                      | 11200          | NSP6                         | 99.693               |
| hsa-miR-1262    | 17                                     | 10   | 5                                   | 22   | 22                                 | 13.829    | 16039                                      | 16060          | RdRp                         | 99.558               |
| hsa-miR-23a-3p  | 17                                     | 8  | 4                                   | 21   | 21                                 | 13.829    | 20754                                      | 20774          | 2-O-RMT                      | 99.347               |
| hsa-miR-6745    | 17                                     | 8  | 4                                   | 21   | 21                                 | 13.829    | 24369                                      | 24389          | spike                        | 98.837               |
| hsa-miR-6822-3p | 18                                     | 11   | 6                                   | 24   | 24                                 | 13.712    | 243  | 266            | 5'-UTR                       | 99.683               |
| hsa-miR-374a-3p | 16                                     | 12   | 6                                   | 22   | 22                                 | 13.591    | 21848                                      | 21869          | spike                        | 98.107               |
| hsa-miR-187-3p  | 16                                     | 12   | 6                                   | 22   | 22                                 | 13.591    | 28377                                      | 28398          | nucleocapsid                 | 98.962               |
| hsa-miR-4320    | 14                                     | 9  | 4                                   | 18   | 18                                 | 13.530    | 10339                                      | 10356          | 3CL-Pro                      | 99.789               |

(c) number of nucleotide mismatches between the human miRNA and the SARS-CoV-2 genome, and (d) the difference in the length before and after alignment of the human miRNA. From 2656 ranked miRNAs, the top 20 human miRNAs are considered, which target different coding and non-coding regions of the SARS-CoV-2 genome. Moreover, molecular docking of such human miRNAs with virus mRNA is performed to verify the efficacy of the interactions. Furthermore, out of the top 20, four human miRNAs like hsa-miR-3611, hsa-miR-1262, hsa-miR-3121-3p, and hsa-miR-4320 are identified to have the seed region. In order to inhibit the virus, the key human targets of the seed regions may be targeted. For this purpose, drugs like carfilzomib, bortezomib, hydralazine, and paclitaxel are identified for such purpose.

## MATERIALS AND METHODS

In this section, the details of data acquisition and preparation are described along with a brief discussion on the pipeline of the proposed work.

**Data Acquisition.** The reference genome (NC\_045512.2) of the SARS-CoV-2 virus is collected from the National Center for Biotechnology Information (NCBI)<sup>1</sup>, followed by the collection of 2656 human miRNAs in fasta format from miRBase2. For alignment purpose, Clustal Omega is used. Please note that for the alignment of sequences, the High-Performance Computing (HPC) facility of NITTTR, Kolkata, is used. The HPC cluster has a master node with a dual Intel Xeon Gold 6130 processor having 32 cores, 2.10 GHz, 22 MB L3 cache, 128 GB DDR4 RAM, and 2 GPU and 4 CPU computing nodes with a dual Intel Xeon Gold 6152 processor having 44 cores, 2.1 GHz, 30 MB L3 cache, and 192 GB DDR4 RAM each, while GPU nodes have Nvidia Tesla V100 GPU with 16 GB memory each.

**Pipeline of the Work.** The pipeline of the work is given in Figure 1a. Initially, the complement of 2656 human miRNAs is computed, as the complement binds to human or virus mRNA. Thereafter, they are aligned with respect to the reference genome of SARS-CoV-2 (NC-045512.2) using the Clustal Omega (ClustalO)<sup>31</sup> alignment technique. Clustal Omega is the new addition to the Clustal multiple sequence alignment family and has increased scalability, thereby facilitating thousands of sequence alignments quickly due to the HMM probabilistic model while taking care of the evolutionary changes in a set of sequences through capturing position-specific patterns. In Clustal Omega, updated mBed is taken into account with a complexity of  $O(d \log N)$ , where mBed refers to embedding layer of “ $d$ ” dimension representing each sequence and “ $d$ ” is proportional to “ $\log N$ ”. Hence, each  $n$ -dimensional vector represents each sequence. Each of these sequences can be clustered with the help of K-means and UPGMA methods. Thus, due to such advantage of aligning large sequences quickly by considering the evolutionary patterns, Clustal Omega is used for alignment in this work. Once the alignment is done, the ranking of each human miRNAs is performed with the help of a new scoring function as given in eq 1.

$$S = \log_2 \left( \frac{m \times c}{n} \right) \times e^{1/(\lambda - \delta) + 1} \quad (1)$$

where  $S$  denotes the score of each miRNA,  $m$  represents the total number of nucleotide matches between human miRNA and the SARS-CoV-2 genome,  $c$  represents the number of consecutive nucleotide matches between human miRNA and the SARS-CoV-2 genome,  $n$  represents the number of nucleotide mismatches between the human miRNA and the SARS-CoV-2 genome, and the difference in the length before ( $\delta$ ) and after ( $\lambda$ ) alignment of the miRNA is given by  $\lambda - \delta$ . The purpose of



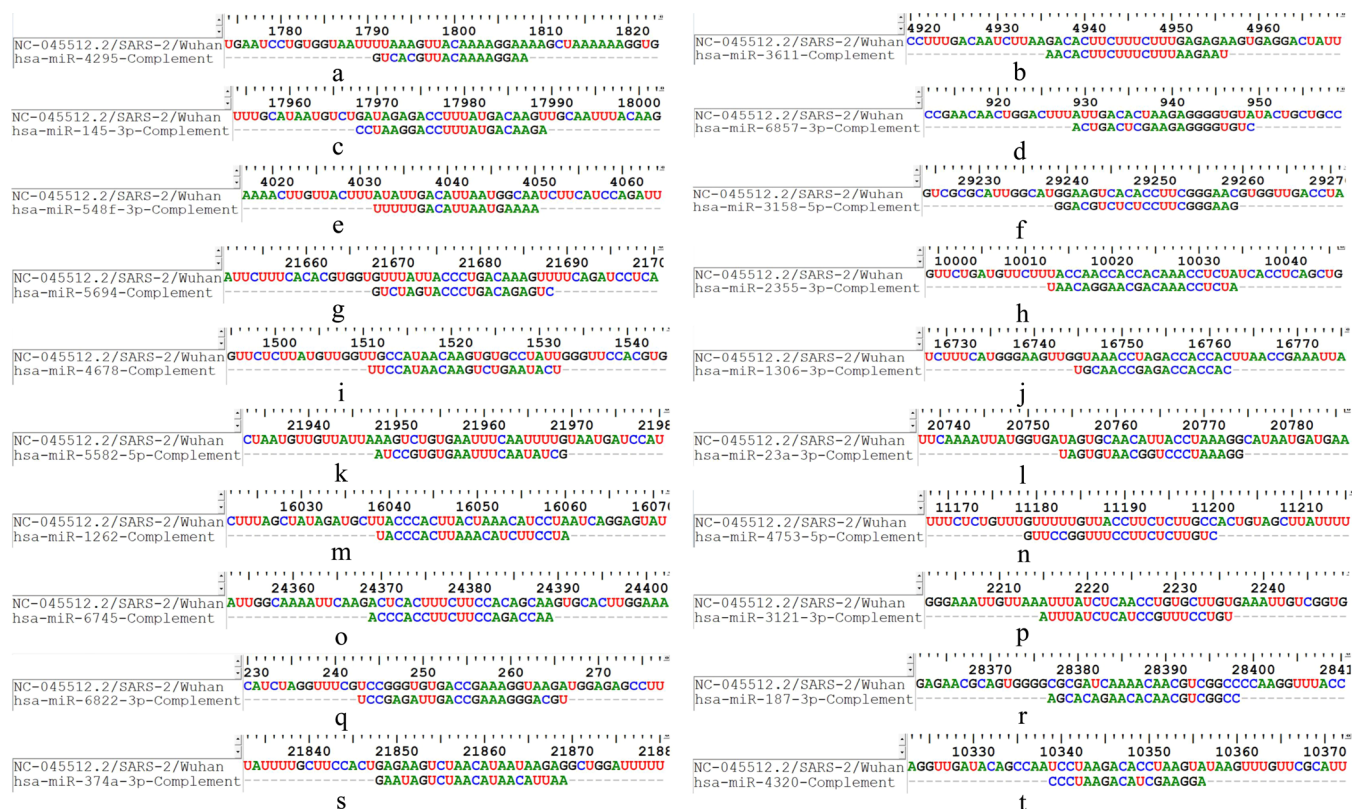


**Figure 2.** Aligned SARS-CoV-2 genome with complements of (a) hsa-miR-4295 (b) hsa-miR-3611 (c) hsa-miR-145-3p (d) hsa-miR-6857-3p (e) hsa-miR-548f-3p (f) hsa-miR-3158-5p (g) hsa-miR-5694 (h) hsa-miR-2355-3p (i) hsa-miR-4678 (j) hsa-miR-1306-3p (k) hsa-miR-5582-5p (l) hsa-miR-23a-3p (m) hsa-miR-1262 (n) hsa-miR-4753-5p (o) hsa-miR-6745 (p) hsa-miR-3121-3p (q) hsa-miR-6822-3p (r) hsa-miR-187-3p (s) hsa-miR-374a-3p (t) hsa-miR-4320, human miRNAs with the help of ClustalO.

defining the scoring function in this way is to consider the influence of all the relative parameters. e.g.,  $m$  and  $c$  should be higher while,  $n$  and  $\lambda - \delta$  should be smaller to have relevant miRNAs as proper binders. After the scoring of each miRNA, the top 20 human miRNAs are selected for further biological validations. In this regard, molecular docking of such human miRNAs with virus mRNA is performed using HNADOCK<sup>32</sup> to verify the efficacy of the interactions. In addition to this, the characteristics of these 20 miRNAs are shown after performing KEGG pathway analysis using the Enrichr tool<sup>33–35</sup> with the top human targets from miRDB.<sup>36</sup>

## RESULTS AND DISCUSSION

The results of this work are obtained after executing the pipeline as shown in Figure 1a. This study focuses on the selection of miRNAs whose complement can bind effectively to the SARS-CoV-2 genome in order to inhibit the viral replication and thereby degrading the functionality of viral proteins. In this regard, complement of 2656 human miRNAs is aligned with the virus genome or mRNA in order to identify sites of possible interactions. The aligned sequences are provided in the supplementary. After alignment, all the human miRNAs are ranked in order to identify the best candidates, which can have a vital role in inhibiting the virus genome. The top 20 ranked miRNAs are reported in Table 1 while the rest are given in the supplementary as Table S1. Also, the aligned 20 such complemented miRNAs with the reference SARS-CoV-2 genome are shown in Figure 2. Please note that in Figure 2, “SAR-2/Wuhan” is “SARS-CoV-2 isolate Wuhan-hu-1”. The naming convention is taken from the NCBI.

**Table 2.** Binding Affinity and RMSD of Such Top 20 Human miRNAs after Docking with the Reference SARS-CoV-2 Genome

| human miRNA     | binding affinity | human miRNA     | binding affinity |
|-----------------|------------------|-----------------|------------------|
| hsa-miR-4295    | −313.65          | hsa-miR-5582-5p | −192.96          |
| hsa-miR-3611    | −239.16          | hsa-miR-23a-3p  | −214.28          |
| hsa-miR-145-3p  | −314.77          | hsa-miR-1262    | −262.11          |
| hsa-miR-6857-3p | −259.74          | hsa-miR-4753-5p | −107.05          |
| hsa-miR-548f-3p | −301.88          | hsa-miR-6745    | −229.92          |
| hsa-miR-3158-5p | −321.43          | hsa-miR-3121-3p | −535.09          |
| hsa-miR-5694    | −283.65          | hsa-miR-6822-3p | −230.78          |
| hsa-miR-2355-3p | −332.23          | hsa-miR-187-3p  | −318.65          |
| hsa-miR-4678    | −261.47          | hsa-miR-374a-3p | −329.32          |
| hsa-miR-1306-3p | −259.07          | hsa-miR-4320    | −431.48          |

As can be seen from Table 1, the top 20 human miRNAs are prone to bind with several coding regions of SARS-CoV-2 reference genome like NSP2, NSP3, helicase, nucleocapsid, spike, NSP4, 2'-O-RMT, RdRp, NSP6, and 3CL-Pro as well as a non-coding region like 5'-UTR. With a score ( $S$ ) of 16.37, which is calculated considering eq 1, hsa-miR-4295 is the top human miRNA prone to bind with SARS-CoV-2 coding region NSP2. Moreover, the conservativeness of the binding regions of the SARS-CoV-2 genome is also computed. In this regard, target regions of the SARS-CoV-2 genome of the top 20 human miRNAs are verified in 10407 SARS-CoV-2 genomes and subsequently reported in Table 1. For example, the genomic coverage of hsa-miR-4295 is 99.88%.

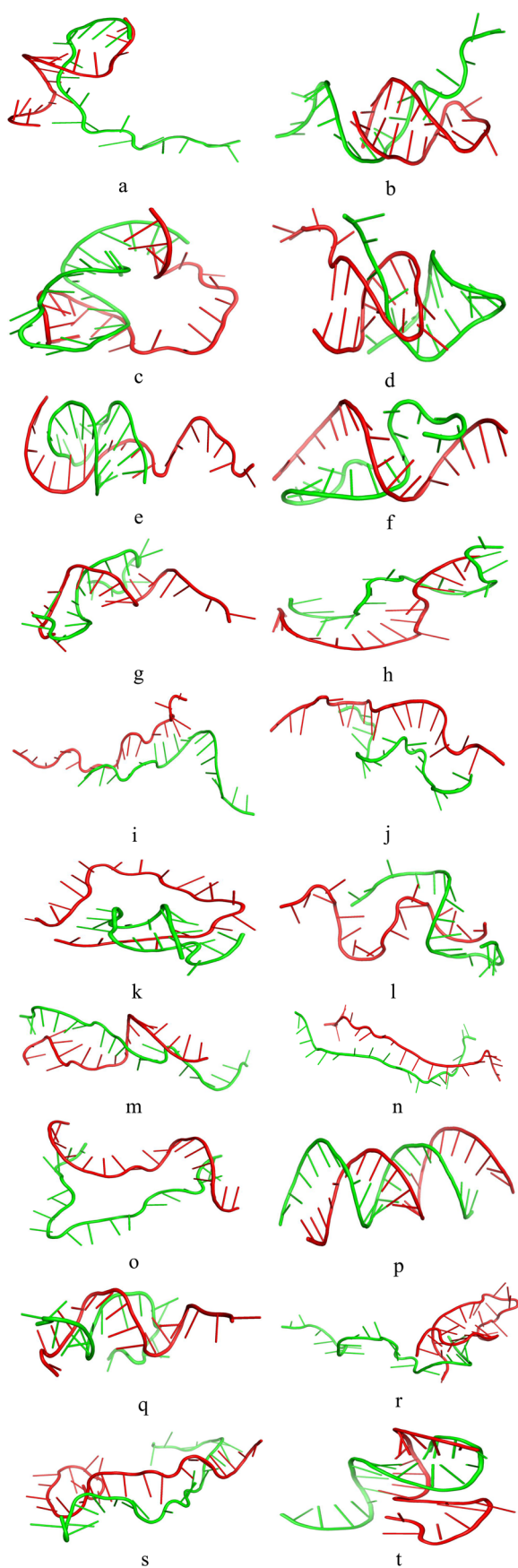


**Figure 3.** Docked poses of (a) hsa-miR-4295 (b) hsa-miR-3611 (c) hsa-miR-145-3p (d) hsa-miR-6857-3p (e) hsa-miR-548f-3p (f) hsa-miR-3158-5p (g) hsa-miR-5694 (h) hsa-miR-2355-3p (i) hsa-miR-

**Figure 3.** continued

4678 (j) hsa-miR-1306-3p (k) hsa-miR-5582-5p (l) hsa-miR-23a-3p (m) hsa-miR-1262 (n) hsa-miR-4753-5p (o) hsa-miR-6745 (p) hsa-miR-3121-3p (q) hsa-miR-6822-3p (r) hsa-miR-187-3p (s) hsa-miR-374a-3p (t) hsa-miR-4320, human miRNAs into the SARS-CoV-2 regions.

Notably, as can be seen from Table 1, hsa-miR-5694, hsa-miR-5582-5p, hsa-miR-6745, and hsa-miR-374a-3p are able to bind to the spike coding region of the SARS-CoV-2 genome, wherein spike glycoprotein plays a vital role in the infection by helping the virus to enter the human cell through ACE2 receptors.<sup>37</sup> Hence, the identified putative miRNAs that bind to the spike gene of SARS-CoV-2 may be considered for further study. Moreover, it is found that NSP2 plays a vital role in viral replication by binding to the host cells. Cornillez-Ty et al.<sup>38</sup> have found the presence of four putative trans-membrane helices along with an amino acid substitution that may result in an increased infectivity of the virus. From the table, it can be seen that highest ranked miRNA that is miR-4295, which lies in the intron region of the VTI1A gene, plays as an inhibitor for the SARS-CoV-2 genome in the NSP2 coding region. It is also found that miR-4295 plays a role in inhibiting cancers.<sup>39</sup> On the other hand, hsa-miR-3611, the second highest scoring miRNA, targets the NSP3 coding region, which is known to hinder host response and contribute to the virus' pathogenesis in the host body. Furthermore, another top scoring human miRNA hsa-miR-145-3p, which functions as a tumour suppressor in the case of head and neck squamous cell carcinoma,<sup>40</sup> targets the helicase coding region. Also, nucleocapsid protein plays multiple roles in the infection of SARS-CoV-2 through binding and packaging of the viral RNA. From the table, it can be seen that hsa-miR-3158-3p and hsa-miR-187-3p, which work as cancer inhibitors, target this region. Therefore, they can possibly play a vital role in inhibiting the SARS-CoV-2 virus as well.

Furthermore, the binding efficacy of the top 20 miRNAs with the virus genome is verified by docking, which is reported in Table 2 and visualised in Figure 3. In Figure 3, the docked poses of the miRNAs are shown in red while the virus mRNA (genome) is shown in green. e.g., the binding affinity score of hsa-miR-4295 is  $-313.65$ ; a negative value shows more binding efficacy.

As a further study, to identify the potential illnesses associated with the identified human miRNAs, KEGG pathway analysis was also carried out by considering their targets, and the results are reported in Table 3. It can be observed from the table that the identified human miRNAs play important roles in various diseases like hepatocellular carcinoma (FDR corrected  $p$ -value  $2.81 \times 10^{-1}$ ), type-II diabetes mellitus (FDR corrected  $p$ -value  $4.16 \times 10^{-1}$ ), axon guidance (FDR corrected  $p$ -value  $6.73 \times 10^{-1}$ ), maturity onset diabetes of the young (FDR corrected  $p$ -value  $6.81 \times 10^{-1}$ ), and ErbB signaling pathway (FDR corrected  $p$ -value  $6.90 \times 10^{-1}$ ). These results are provided in the supplementary.

Please note that the seed region of miRNA is mostly situated at positions 2–7 from the miRNA 5'-end. The seed sequence is essential for the binding of the miRNA to the mRNA. In Figure 2, miRNAs like hsa-miR-3611 (b), hsa-miR-1262 (m), hsa-miR-3121-3p (p), and hsa-miR-4320 (t) have the seed regions out of the 20 listed miRNAs. Viruses usually use this seed region for survival. It can be seen from<sup>41</sup> that upon binding with miR-122, which is in the seed region, translation and initiation of

Table 3. KEGG Pathway Analysis of the Top 20 Human miRNAs Based on the Key Human Targets

| human miRNAs    | targets                               | KEGG pathways                        | FDR corrected p-value | human miRNAs    | targets                               | KEGG pathways                                    | FDR corrected p-value |
|-----------------|---------------------------------------|--------------------------------------|-----------------------|-----------------|---------------------------------------|--|-----------------------|
| hsa-miR-4295    | BRCA1, CREBBP, CCNH, RPA3, HIF1A      | homologous recombination             | $3.07 \times 10^{-1}$ | hsa-miR-5582-5p | PPP2R1A, ARID4B, SRSF3, BAZ2A, CEBPD  | synaptic vesicle cycle                           | $2.31 \times 10^{-1}$ |
|                 | GTF2A1, UBQLN2, C1orf162, CBX5, RBBP5 | basal transcription factors          | $3.07 \times 10^{-1}$ |                 | CHD6, FNDC3B, GPC6, MED13L, NFIB      | hippo signaling pathway                          | $1.42 \times 10^{-1}$ |
|                 |                                       | nucleotide excision repair           | $3.07 \times 10^{-1}$ |                 |                                       | chagas disease                                   | $1.75 \times 10^{-1}$ |
|                 |                                       | fanconi anemia pathway               | $3.07 \times 10^{-1}$ |                 |                                       | dopaminergic synapse                             | $2.29 \times 10^{-1}$ |
|                 |                                       | notch signaling pathway              | $3.07 \times 10^{-1}$ |                 |                                       | adrenergic signaling in cardiomyocytes           | $2.29 \times 10^{-1}$ |
| hsa-miR-3611    | PSMB1, PSMB6, PSMC4, PSMA2, PSMA4     | Th17 cell differentiation            | $1.95 \times 10^{-1}$ | hsa-miR-23a-3p  | HDAC2, FBXL3, CBX5, RFX5, YOD1        | chronic myeloid leukemia                         | $1.09 \times 10^{-1}$ |
|                 | PSMA8, PPP3R1, UBE2E3                 | spinocerebellar ataxia               | $1.95 \times 10^{-1}$ |                 | TGS1, SPOPL, SH2B3, SCN1B, RUNX1      | Th17 cell differentiation                        | $1.46 \times 10^{-1}$ |
|                 |                                       | axon guidance                        | $2.06 \times 10^{-1}$ |                 |                                       | cell adhesion molecules                          | $1.72 \times 10^{-1}$ |
|                 |                                       | prion disease                        | $2.06 \times 10^{-1}$ |                 |                                       | human papillomavirus infection                   | $1.72 \times 10^{-1}$ |
|                 |                                       | circadian rhythm                     | $2.06 \times 10^{-1}$ |                 |                                       | PI3K-Akt signaling pathway                       | $1.72 \times 10^{-1}$ |
| hsa-miR-145-3p  | NOTCH1, PAX5, ATLL1, CD40LG, CERKL    | PPAR signaling pathway               | $4.92 \times 10^{-1}$ | hsa-miR-1262    | UBB, HIP1, DAB2, GNG13, BMP2          | hepatocellular carcinoma                         | $5.30 \times 10^{-1}$ |
|                 | DLG5, GTF2I, NCAPG, NKX3-1, RAB10     | Fc gamma R-mediated phagocytosis     | $4.92 \times 10^{-1}$ |                 | CBLB, HTR2C, INTS2, POLI, PRKCE       | fatty acid elongation                            | $2.52 \times 10^{-1}$ |
|                 |                                       | AMPK signaling pathway               | $4.92 \times 10^{-1}$ |                 |                                       | glycosaminoglycan biosynthesis                   | $3.21 \times 10^{-1}$ |
|                 |                                       | breast cancer                        | $4.92 \times 10^{-1}$ |                 |                                       | cushing syndrome                                 | $3.21 \times 10^{-1}$ |
|                 |                                       | cell adhesion molecules              | $4.92 \times 10^{-1}$ |                 |                                       | basal cell carcinoma                             | $3.27 \times 10^{-1}$ |
| hsa-miR-6857-3p | PIK3CA, TP53BP1, CHD3, ARID1A, SNW1   | hepatocellular carcinoma             | $2.81 \times 10^{-1}$ | hsa-miR-4753-5p | PIK3R3, SIAH1, UBE2J, IGFBP5, INHBB   | Fc gamma R-mediated phagocytosis                 | $2.07 \times 10^{-1}$ |
|                 | E2F3, SMARCD1, ARID2, AR, RELN        | type II diabetes mellitus            | $4.16 \times 10^{-1}$ |                 | LRRG5, NOAI, OLIG1, EPHA3, PLCXD3     | Ras signaling pathway                            | $2.07 \times 10^{-1}$ |
|                 |                                       | axon guidance                        | $6.73 \times 10^{-1}$ |                 |                                       | shigellosis                                      | $2.07 \times 10^{-1}$ |
|                 |                                       | maturity onset diabetes of the young | $6.81 \times 10^{-1}$ |                 |                                       | autophagy  | $2.07 \times 10^{-1}$ |
| hsa-miR-548f-3p | ACTB, AGO2, PRKACA, CSNK1A1, MECP2    | ErbB signaling pathway               | $6.90 \times 10^{-1}$ | hsa-miR-6745    | CREBBP, ARID1B, HDAC3, KDM6A, SMAD2   | ubiquitin mediated proteolysis                   | $2.07 \times 10^{-1}$ |
|                 | YWHA8, KLRD1, ADCY9, TUBB6, RUNX1     | gastric acid secretion               | $3.45 \times 10^{-2}$ |                 | SMURF2, AGO3, CCDC135, CLTCL1, NDFIPI | inflammatory mediator regulation of TRP channels | $4.74 \times 10^{-1}$ |
|                 |                                       | <i>Vibrio cholerae</i> infection     | $7.44 \times 10^{-2}$ |                 |                                       | hedgehog signaling pathway                       | $2.64 \times 10^{-2}$ |
|                 |                                       | oxytocin signaling pathway           | $1.49 \times 10^{-1}$ |                 |                                       | TGF-beta signaling pathway                       | $5.96 \times 10^{-2}$ |
|                 |                                       | tight junction                       | $1.49 \times 10^{-1}$ |                 |                                       | hippo signaling pathway                          | $1.86 \times 10^{-1}$ |
|                 |                                       | gap junction                         | $1.49 \times 10^{-1}$ |                 |                                       | adherens junction                                | $2.31 \times 10^{-1}$ |
| hsa-miR-3158-5p | CUL3, ASB13, LSM14A, KLHL42, UBE2B    | oxytocin signaling pathway           | $5.83 \times 10^{-1}$ | hsa-miR-3121-3p | CHST12, EXOSC6, ANAPC2, CERK, EPHA7   | hepatitis C                                      | $2.29 \times 10^{-1}$ |
|                 | CADM2, TIA1, COPS7B, HNRNPR, PRKCA    | aldosterone synthesis and secretion  | $5.83 \times 10^{-1}$ |                 | ERC1, GNE, HS6ST1, KBTBD13, LSM2      | glycosaminoglycan biosynthesis                   | $4.32 \times 10^{-1}$ |
|                 |                                       | vascular smooth muscle contraction   | $5.83 \times 10^{-1}$ |                 |                                       | RNA degradation                                  | $4.32 \times 10^{-1}$ |
|                 |                                       | spinocerebellar ataxia               | $5.83 \times 10^{-1}$ |                 |                                       | NF-kappa B signaling pathway                     | $4.32 \times 10^{-1}$ |
|                 |                                       | notch signaling pathway              | $5.83 \times 10^{-1}$ |                 |                                       | ubiquitin mediated proteolysis                   | $4.32 \times 10^{-1}$ |

Table 3. continued

| human miRNAs    | targets  | KEGG pathways  | FDR corrected p-value   | human miRNAs    | targets   | KEGG pathways  | FDR corrected p-value  |
|-----------------|--|--|---|-----------------|---|--|--|
| hsa-miR-5694    | TRIP12, YWHAE, FGB, RAB1A, KIA1A<br>GSPT1, PABPC3, SMG6, SYP, TOM1L2   | mRNA surveillance pathway<br>gap junction<br>inflammatory mediator regulation of TRP channels<br>endocytosis<br>serotonergic synapse   | $2.86 \times 10^{-1}$<br>$5.59 \times 10^{-1}$<br>$5.59 \times 10^{-1}$<br>$5.59 \times 10^{-1}$<br>$5.59 \times 10^{-1}$   | hsa-miR-6822-3p | CREBBP, CCNA2, SSB, OGT, SNRPC<br>UBE2D1, YBX1, CDK17, GFPT1, PLIN1       | protein export<br>cell cycle<br>insulin resistance<br>hepatitis B<br>protein processing in endoplasmic reticulum   | $4.32 \times 10^{-1}$<br>$1.09 \times 10^{-1}$<br>$3.60 \times 10^{-1}$<br>$3.60 \times 10^{-1}$<br>$3.60 \times 10^{-1}$  |
| hsa-miR-2355-3p | VAMP2, IL2RG, TXN2, SV2B, STMN2<br>NXN, NSD1, NR6A1, KDM6A, ATXN1      | arrhythmic right ventricular cardiomyopathy<br>cardiac muscle contraction  | $1.33 \times 10^{-1}$<br>$1.33 \times 10^{-1}$  | hsa-miR-187-3p  | MECP2, STRBP, ELAVL2, GNL3L, MAPK1<br>ADAMTSS, RAPIA, PAPOLG, MTM1, MMP15 | sphingolipid signaling pathway<br>neurotrophin signaling pathway   | $4.47 \times 10^{-1}$<br>$2.89 \times 10^{-2}$   |
| hsa-miR-4678    | TNPO1, PSMD1, DKC1, GRIN3A, TAOK1<br>STK4, RFC5, PPP3R1, OPRM1, NOTUM  | hypertrophic cardiomyopathy<br>NOD-like receptor signaling pathway<br>dilated cardiomyopathy<br>prion disease<br>MAPK signaling pathway<br>spinocerebellar ataxia<br>Wnt signaling pathway<br>glutamatergic synapse<br>non-alcoholic fatty liver disease | $1.33 \times 10^{-1}$<br>$1.33 \times 10^{-1}$<br>$1.33 \times 10^{-1}$<br>$6.40 \times 10^{-2}$<br>$6.40 \times 10^{-2}$<br>$9.78 \times 10^{-2}$<br>$1.25 \times 10^{-1}$<br>$2.46 \times 10^{-1}$<br>$1.09 \times 10^{-1}$ | hsa-miR-374a-3p | FOXP3, FOXP4, HDLBP, IREB2, LATS2<br>LSAMP, NEGR1, NEFAT5, PAPOLG, RORA   | renal cell carcinoma<br>ErbB signaling pathway<br>focal adhesion<br>ras signaling pathway<br>cell adhesion molecules<br>axon guidance<br>inflammatory bowel disease<br>Th17 cell differentiation<br>FoxO signaling pathway | $4.56 \times 10^{-2}$<br>$5.19 \times 10^{-2}$<br>$5.19 \times 10^{-2}$<br>$7.00 \times 10^{-2}$<br>$1.27 \times 10^{-1}$<br>$1.27 \times 10^{-1}$<br>$2.43 \times 10^{-1}$<br>$4.21 \times 10^{-1}$ |
| hsa-miR-1306-3p | ELAVL2, NOVA1, INSR, NRXN1, NR1D2<br>NCOR2, ANKRD34A, SPEN, SOX2, SNX1 | non-alcoholic fatty liver disease<br>arginine and proline metabolism<br>Fa nconi anemia pathway<br>protein processing in endoplasmic reticulum<br>diabetic cardiomyopathy  | $1.09 \times 10^{-1}$<br>$3.18 \times 10^{-1}$<br>$3.18 \times 10^{-1}$<br>$3.18 \times 10^{-1}$<br>$3.18 \times 10^{-1}$   | hsa-miR-4320    | RHOA, GNG13, PRKCA, PLXNA4, TBC1D2B<br>CCRI, CSDE1, EFNB3, CBFA2T3, PNOC  | axon guidance<br>morphine addiction<br>human cytomegalovirus infection<br>sphingolipid signaling pathway   | $8.22 \times 10^{-2}$<br>$8.22 \times 10^{-2}$<br>$8.22 \times 10^{-2}$<br>$8.22 \times 10^{-2}$   |



Table 4. Drugs Targeting the Key Human Targets of the Seed Regions

| miRNA           | genes                             | drugs               | treatment  | DrugBank ID |
|-----------------|-----------------------------------|---------------------|--|-------------|
| hsa-miR-3611    | PSMB6, PSMA4, PSMA2, PSMB1, PSMA8 | carfilzomib         | multiple myeloma   | DB08889     |
|                 | PSMB6, PSMA4, PSMA2, PSMB1, PSMA8 | bortezomib          | multiple myeloma   | DB00188     |
|                 | PSMB6, PSMA4, PSMA2, PSMB1        | hydralazine         | hypertension   | DB01275     |
|                 | PSMB6, PSMA4, PSMB1               | paclitaxel          | carcinoma of the ovary, and other various cancers including breast and lung cancer   | DB01229     |
| hsa-miR-1262    | HTR2C, POLI                       | clozapine           | schizophrenia  | DB00363     |
|                 | BMP2, HIP1, HTR2C, POLI           | metronidazole       | trichomoniasis, amebiasis, inflammatory lesions of rosacea and bacterial infections, as well as prevent postoperative infections | DB00916     |
|                 | HTR2C                             | mirtazapine         | major depression   | DB00370     |
|                 | HTR2C                             | trazodone           | major depression   | DB00656     |
| hsa-miR-3121-3p | CERK                              | niclosamide         | treatment of beef, pork, fish, and dwarf tapeworm infections   | DB06803     |
|                 | CHST12                            | tanespimycin        | several types of cancer, solid tumors or chronic myelogenous leukemia  | DB05134     |
|                 | CERK, CHST12                      | azacitidine         | myelodysplastic syndrome   | DB00928     |
|                 | CHST12                            | etoposide           | testicular and small cell lung tumors  | DB00773     |
| hsa-miR-4320    | CSDE1, PRKCA                      | tetrahydropalmatine | under investigation in clinical trial for the treatment of schizophrenia   | DB12093     |
|                 | EFNB3, PRKCA, RHOA                | doxorubicin         | cancers and Kaposi's sarcoma   | DB00997     |
|                 | CCR1, CBFA2T3                     | niclosamide         | treatment of beef, pork, fish, and dwarf tapeworm infections   | DB06803     |
|                 | PRKCA                             | mianserin           | depression and anxiety   | DB06148     |

replication for hepatitis C virus are increased. Thus, in order to inhibit the virus, the key human targets of the seed regions may be targeted. Table 4 reports some repurposable drugs for the same. For example, the key genes of hsa-miR-3611 can be targeted by drugs like carfilzomib, bortezomib, hydralazine, and paclitaxel to inhibit the virus infection. It is to be noted that the target regions of the SARS-CoV-2 genome are mostly conserved. Also, all the mutations in the different strains of SARS-CoV-2 have been checked and there are no changes in those positions where the 20 miRNAs target the SARS-CoV-2 genome. Thus, the current mutant strains have the same sequences that could interact with the reported top 20 human miRNAs.

## CONCLUSIONS

In this work, a new approach has been hypothesized for identifying miRNAs that can inhibit the SARS-CoV-2 genome. Therefore, to find the putative miRNA biomarkers, we have proposed a new scoring function after considering the alignment of 2656 miRNAs with respect to the virus genome. The scoring function is defined based on different parameters like the total number of nucleotide matches between the human miRNA and the SARS-CoV-2 genome, the number of consecutive nucleotide matches between the human miRNA and the SARS-CoV-2 genome, the number of nucleotide mismatches between the human miRNA and the SARS-CoV-2 genome, and the difference in the length before and after alignment of the human miRNA. As a result, the top 20 miRNAs as biomarkers are identified, which bind to the various SARS-CoV-2 coding and non-coding regions, thereby possibly working as inhibitors of SARS-CoV-2. Moreover, to verify the efficacy of the interactions, molecular docking of such human miRNAs with virus mRNA is performed and promising results are found and discussed. Therefore, the identified miRNAs may work as putative biomarkers for inhibiting the SARS-CoV-2 virus. Out of the 20 identified miRNAs, 4 miRNAs have the seed region. Thus, drugs such as paclitaxel, bortezomib, carfilzomib, and hydralazine that may inhibit virus infection are identified for the human targets of these four miRNAs.

## ASSOCIATED CONTENT

### Supporting Information

The Supporting Information is available free of charge at <https://pubs.acs.org/doi/10.1021/acsomega.2c05091>.

List of 2656 human miRNAs targeting SARS-CoV-2 genome in different coding and non-coding regions (PDF)

## AUTHOR INFORMATION

### Corresponding Authors

**Indrajit Saha** – Department of Computer Science and Engineering, National Institute of Technical Teachers' Training and Research, Kolkata 700106 West Bengal, India; Email: [indrajit@nittrkol.ac.in](mailto:indrajit@nittrkol.ac.in)

**Nimisha Ghosh** – Department of Computer Science and Information Technology, Institute of Technical Education and Research, Siksha "O" Anusandhan (Deemed to be) University, Bhubaneswar 751030 Odisha, India; [orcid.org/0000-0002-0697-6368](https://orcid.org/0000-0002-0697-6368); Email: [ghosh.nimisha@gmail.com](mailto:ghosh.nimisha@gmail.com)

**Dariusz Plewczynski** – Laboratory of Bioinformatics and Computational Genomics, Faculty of Mathematics and Information Science, Warsaw University of Technology, Warsaw 00-661, Poland; Laboratory of Functional and Structural Genomics, Centre of New Technologies, University of Warsaw, Warsaw 02-097, Poland; Email: [d.plewczynski@cent.uw.edu.pl](mailto:d.plewczynski@cent.uw.edu.pl)

Complete contact information is available at: <https://pubs.acs.org/doi/10.1021/acsomega.2c05091>

### Author Contributions

<sup>1</sup>N.G. contributed equally.

### Funding

This work was supported by the CRG short-term research grant on COVID-19 (CVD/2020/000991) from the Science and Engineering Research Board (SERB), Department of Science and Technology, Govt. of India. This work was co-funded by Warsaw University of Technology within the Excellence



Initiative: Research University (IDUB) programme. This work was been co-supported by the Polish National Science Centre (2019/35/O/ST6/02484 and 2020/37/B/NZ2/03757).

## Notes

The authors declare no competing financial interest. Ethics approval or individual consent is not applicable. The supplementary of this work is available at "<http://www.nittrkol.ac.in/indrajit/projects/COVID-Human-miRNA-SARS-CoV-2-Interactions/>".

## ACKNOWLEDGMENTS

We thank all those who have contributed sequences to the GISAID database.

## REFERENCES

- (1) Zhang, S.; Amahong, K.; Sun, X.; Lian, X.; Liu, J.; Sun, H.; Lou, Y.; Zhu, F.; Qiu, Y. The miRNA: a small but powerful RNA for COVID-19. *Briefings Bioinf.* **2021**, *22*, 1137–1149.
- (2) Ding, Y.; Jiang, L.; Tang, J.; Guo, F. Identification of human microRNA-disease association via hypergraph embedded bipartite local model. *Comput. Biol. Chem.* **2020**, *89*, 107369.
- (3) Liang, G.; Wu, J.; Xu, L. A prognosis-related based method for miRNA selection on liver hepatocellular carcinoma prediction. *Comput. Biol. Chem.* **2021**, *91*, 107433.
- (4) Acunzo, M.; Romano, G.; Wernicke, D.; Croce, C.-M. MicroRNA and cancer—A brief overview. *Adv. Biol. Regul.* **2015**, *57*, 1–9.
- (5) Bartel, D. P. MicroRNAs. *Cell* **2004**, *116*, 281–297.
- (6) El-Nabi, S. H.; Elhiti, M.; El-Sheekh, M. A New Approach for COVID-19 Treatment by Micro-RNA. *Med. Hypotheses* **2020**, *143*, 110203.
- (7) Girardi, E.; López, P.; Pfeffer, S. On the Importance of Host MicroRNAs During Viral Infection. *Front. Genet.* **2018**, *9*, 439.
- (8) Scheel, T. K.; Luna, J. M.; Liniger, M.; Nishiuchi, E.; Rozen-Gagnon, K.; Shlomai, A.; Auray, G.; Gerber, M.; Fak, J.; Keller, I.; et al. A Broad RNA Virus Survey Reveals Both miRNA Dependence and Functional Sequestration. *Cell Host Microbe* **2016**, *19*, 409–423.
- (9) Luna, J. M.; Scheel, T. K. H.; Danino, T.; Shaw, K. S.; Mele, A.; Fak, J. J.; Nishiuchi, E.; Takacs, C. N.; Catanese, M. T.; de Jong, Y. P.; et al. Hepatitis C virus RNA functionally sequesters miR-122. *Cell* **2015**, *160*, 1099–1110.
- (10) Libri, V.; Helwak, A.; Miesen, P.; Santhakumar, D.; Borger, J. G.; Kudla, G.; Grey, F.; Tollervey, D.; Buck, A. H. Murine cytomegalovirus encodes a miR-27 inhibitor disguised as a target. *Biol. Sci.* **2011**, *109*, 279–284.
- (11) Fani, M.; Zandi, M.; Rezayi, M.; Khodadad, N.; Langari, H.; Amiri, I. The Role of microRNAs in the Viral Infections. *Curr. Pharm. Des.* **2018**, *24*, 4659–4667.
- (12) Balmeh, N.; Mahmoudi, S.; Mohammadi, N.; Karabedianhajiabadi, A. Predicted Therapeutic targets for COVID-19 disease by inhibiting SARS-CoV-2 and its related receptors. *Inform. Med. Unlocked* **2020**, *20*, 100407.
- (13) Li, Q.; Lowey, B.; Sodroski, C.; Krishnamurthy, S.; Alao, H.; Cha, H.; Chiu, S.; El-Diwany, R.; Ghany, M. G.; Liang, T. J. Cellular microRNA networks regulate host dependency of hepatitis C virus infection. *Nat. Commun.* **2017**, *8*, 1789.
- (14) Ho, B.; Yu, S.; Chen, J. J. W.; Chang, S.-Y.; Yan, B.-S.; Hong, Q.-S.; Singh, S.; Kao, C.-L.; Chen, H.-Y.; Su, K.-Y.; et al. Enterovirus-induced miR-141 contributes to shutoff of host protein translation by targeting the translation initiation factor eIF4E. *Cell Host Microbe* **2011**, *9*, 58–69.
- (15) Ingle, H.; Kumar, S.; Raut, A.; Mishra, A.; Kulkarni, D. D.; Kameyama, T.; Takaoka, A.; Akira, S.; Kumar, H. The microRNA miR-485 targets host and influenza virus transcripts to regulate antiviral immunity and restrict viral replication. *Sci. Signal.* **2015**, *8*, ra126.
- (16) Rosenberger, C. M.; Podyminogin, R. L.; Diercks, A. H.; Treuting, P. M.; Peschon, J. J.; Rodriguez, D.; Gundapuneni, M.; Weiss, M. J.; Aderem, A. miR-144 attenuates the host response to influenza virus by targeting the TRAF6-IRF7 signaling axis. *PLoS Pathog.* **2017**, *13*, No. e1006305.
- (17) Roy, S.; Sharma, B.; Mazid, M. I.; Akhand, R. N.; Das, M.; Marufatuzzahan, M.; Chowdhury, T. A.; Azim, K. F.; Hasan, M. Identification and host response interaction study of SARS-CoV-2 encoded miRNA-like sequences: an in silico approach. *Comput. Biol. Med.* **2021**, *134*, 104451.
- (18) Goud, V. R.; Chakraborty, R.; Chakraborty, A.; Lavudi, K.; Patnaik, S.; Sharma, S.; Patnaik, S. A bioinformatic approach of targeting SARS-CoV-2 replication by silencing a conserved alternative reserve of the orf8 gene using host miRNAs. *Comput. Biol. Med.* **2022**, *145*, 105436.
- (19) Islam, M. S.; Khan, M. A.-A.-K. Computational analysis revealed miRNAs produced by Chikungunya virus target genes associated with antiviral immune responses and cell cycle regulation. *Comput. Biol. Chem.* **2021**, *92*, 107462.
- (20) Haldar, A.; Yadav, K. K.; Singh, S.; Yadav, P. K.; Singh, A. K. In silico analysis highlighting the prevalence of BCL2L1 gene and its correlation to miRNA in human coronavirus (HCoV) genetic makeup. *Infect. Genet. Evol.* **2022**, *99*, 105260.
- (21) Zheng, Z.; Ke, X.; Wang, M.; He, S.; Li, Q.; Zheng, C.; Zhang, Z.; Liu, Y.; Wang, H. Human microRNA hsa-miR-296-5p suppresses enterovirus 71 replication by targeting the viral genome. *J. Virol.* **2013**, *87*, 5645–5656.
- (22) Wang, L.; Qin, Y.; Tong, L.; Wu, S.; Wang, Q.; Jiao, Q.; Guo, Z.; Lin, L.; Wang, R.; Zhao, W.; et al. MiR-342-5p suppresses coxsackievirus B3 biosynthesis by targeting the 2C-coding region. *Antiviral Res.* **2012**, *93*, 270–279.
- (23) Lodge, R.; Ferreira Barbosa, J. B.; Lombard-Vadnais, F.; et al. Host MicroRNAs-221 and -222 inhibit HIV-1 entry in macrophages by targeting the CD4 viral receptor. *Cell Rep.* **2017**, *21*, 141–153.
- (24) Wong, R. R.; Noraini, A. A.; Affendi, S.; Poh, C. L. Role of microRNAs in antiviral responses to dengue infection. *J. Biomed. Sci.* **2020**, *27*, 4.
- (25) Betancur, J. C. C.; Inchima, S. U. Overexpression of miR-484 and miR-744 in Vero cells alters Dengue Virus Replication. *Memórias do Inst. Oswaldo Cruz* **2017**, *112*, 281–291.
- (26) Yan, H.; Zhou, Y.; Liu, Y.; Deng, Y.; Puthiyakunnon, X.; Chen, X. miR-252 of the Asian tiger mosquito *Aedes albopictus* regulates dengue virus replication by suppressing the expression of the dengue virus envelope protein. *J. Med. Virol.* **2014**, *86*, 1428–1436.
- (27) Zhu, N.; Zhang, D.; Wang, W.; Li, X.; Yang, B.; Song, J.; Zhao, X.; Huang, B.; Shi, W.; Lu, R.; et al. A Novel Coronavirus from Patients with Pneumonia in China. *N. Engl. J. Med.* **2019**, *382*, 727.
- (28) Rad Sm, A. H.; McLellan, A. Implications of SARS-CoV-2 Mutations for Genomic RNA Structure and Host microRNA Targeting. *Int. J. Mol. Sci.* **2020**, *21*, 4807.
- (29) Arisan, E.; Dart, A.; Grant, G.; Arisan, S.; Cuhadaroglu, S.; Lange, S.; Uysal-Onganer, P. The Prediction of miRNAs in SARS-CoV-2 Genomes: hsa-miR Databases Identify 7 Key miRs Linked to Host Responses and Virus Pathogenicity-Related KEGG Pathways Significant for Comorbidities. *Viruses* **2020**, *12*, 614.
- (30) Chauhan, N.; Jaggi, M.; Chauhan, S.; Yallapu, M. M. COVID-19: Fighting the Invisible Enemy with microRNAs. *Expert Rev. Anti-infect. Ther.* **2020**, *19*, 137–145.
- (31) Sievers, F.; Higgins, D. Clustal Omega. *Curr. Protoc. Bioinf.* **2014**, *48*, 3.13.1–3.13.16.
- (32) He, J.; Wang, J.; Tao, T.; Xiao, S.-Y.; Huang, S. Y. HNADOCK: a nucleic acid docking server for modeling RNA/DNA-RNA/DNA 3D complex structures. *Nucleic Acids Research* **2019**, *47*, W35.
- (33) Chen, E.; Tan, C.; Kou, Y.; Duan, Q.; Wang, Z.; Meirelles, G.; Clark, N.; Ma'ayan, A. Enrichr: Interactive and collaborative HTML5 gene list enrichment analysis tool. *BMC Bioinf.* **2013**, *14*, 128.
- (34) Kulshov, M.; Jones, M.; Rouillard, A.; Fernandez, N.; Duan, Q.; Wang, Z.; Koplev, S.; Jenkins, S.; Jagodnik, K.; Lachmann, A.; McDermott, M.; Monteiro, C.; Gundersen, G.; Ma'ayan, A. Enrichr: A Comprehensive Gene Set Enrichment Analysis Web Server 2016 update. *Nucleic Acids Res.* **2016**, *44*, W90.

(35) Xie, Z.; Bailey, A.; Kuleshov, M.; Clarke, D.; Evangelista, J.; Jenkins, S.; Lachmann, A.; Wojciechowicz, M.; Kropiwnicki, E.; Jagodnik, K.; Jeon, M.; Ma'ayan, A. Gene Set Knowledge Discovery with Enrichr. *Curr. Protoc.* **2021**, *1*, No. e90.

(36) Chen, Y.; Wang, X. MiRDB: An online database for prediction of functional microRNA targets. *Nucleic Acids Res.* **2019**, *48*, D146.

(37) Mariano, G.; Farthing, R.; Lale-Farjat, S.; Bergeron, J. R. C. Structural Characterization of SARS-CoV-2: Where We Are, and Where We Need to Be. *Front. Mol. Biosci.* **2020**, *7*, 605236.

(38) Cornillez-Ty, C. T.; Liao, L.; Yates, J. R.; Kuhn, P.; Buchmeier, M. J. Severe Acute Respiratory Syndrome Coronavirus Nonstructural Protein 2 interacts with a host protein complex involved in mitochondrial biogenesis and intracellular signaling. *J. Virol.* **2009**, *83*, 10314–10318.

(39) Li, Y.; Zhang, Y.; Zou, Y.; Duan, S. The Paradoxical roles of miR-4295 in human cancer: Implications in pathogenesis and personalized medicine. *Genes Dis.* **2020**, *9*, 638.

(40) Yamada, Y.; Koshizuka, K.; Hanazawa, T.; Kikkawa, N.; Okato, A.; Idichi, T.; Arai, T.; Sugawara, S.; Katada, K.; Okamoto, Y.; Seki, N. Passenger strand of miR-145-3p acts as a tumor-suppressor by targeting MYO1B in head and neck squamous cell carcinoma. *Int. J. Oncol.* **2018**, *52*, 166–178.

(41) Schult, P.; Roth, H.; Adams, R. L.; Mas, C.; Imbert, L.; Orlik, C.; Ruggieri, A.; Pyle, A. M.; Lohmann, V. microRNA-122 amplifies hepatitis C virus translation by shaping the structure of the internal ribosomal entry site. *Nature Communications* **2018**, *9*, 2613.